The Use of Probabilistic Modeling for Reentry Thermal Protection System Design

Deepak Bose, Michael J. Wright, and Nagi N. Mansour
NASA Ames Research Center
MS: 230-3, NASA Ames Res. Ctr.
Moffett Field, CA 94035, USA

dbose@mail.arc.nasa.gov

ABSTRACT

An efficient Monte Carlo uncertainty analysis for aerothermal environment modeling of a planetary entry vehicle is performed. The efficiency gain is achieved by using Latin Hypercube Sampling (LHS) instead of traditionally used random sampling. For small sample sizes the results obtained by the LHS technique are shown to be superior in terms of reproducing means and standard deviations. With LHS reasonable values of output uncertainty and sensitivity ranking are obtained with a sample size as small as 100. For thermal protection system design, an efficient sampling technique allows a Monte Carlo analysis to be applied to more complex systems involving three dimensional simulations with coupled physical phenomena.

1. INTRODUCTION

The design of a thermal protection system (TPS) for a planetary entry vehicle relies on ground testing as well as modeling and simulation of flight environment and material response. Modeling is used to define the aerothermal and aerodynamic environments that an entry vehicle will encounter. The environment envelope is then used to define a ground testing program in order to to select, design, and qualify a TPS material. Available ground testing facilities, however, are unable to reproduce many of the environmental parameters deemed critical, which gives rise to ground-to-flight traceability concerns. Modeling and simulation also play the critical role of bridging the ground-to-flight traceability gap. Measured data from tests are used for model development, which usually involves calibration of unknown parameters, required for various phenomenological and physics based models. A thermal protection material generally responds to a variety of flow parameters, such as heat flux (sensible, catalytic, and radiative), pressure, shear stress, turbulence, enthalpy, etc. Adequate modeling requires an in-depth description of various interacting physical and chemical phenomena. Our understanding of these phenomena, and their interactions, vary from excellent to extremely poor. A suite of various approximate and phenomenological models are, therefore, employed. Understandably, the predictions of modeling and simulation of aerothermal environment and material response are not perfect and suffer from uncertainties.

In order to develop design margins and meet TPS reliability requirements, uncertainty in model predictions must be quantified via an uncertainty analysis. An uncertainty analysis identifies the overall prediction uncertainty as well as the primary uncertainty drivers that can be subsequently prioritized and targeted for further testing and investigation or research. A sensitivity analysis, which is a by-product of the uncertainty analysis, provides valuable insights by identifying physical mechanisms that are rate-limiting and must be

Bose, D.; Wright, M.J.; Mansour, N.N. (2007) The Use of Probabilistic Modeling for Reentry Thermal Protection System Design. In *Computational Uncertainty in Military Vehicle Design* (pp. 14-1 – 14-12). Meeting Proceedings RTO-MP-AVT-147, Paper 14. Neuilly-sur-Seine, France: RTO. Available from: http://www.rto.nato.int.

known with greater fidelity. Aerothermal modeling involves the numerical solution of compressible fluid dynamics equations for high speed flows with nonequilibrium chemical kinetics and thermodynamics. Due to the inherent nonlinearities, a Monte Carlo analysis is often carried out in order to analyze the sensitivities and uncertainties inherent in the chosen physical model.

A Monte Carlo sensitivity and uncertainty analysis involves random sampling of all input parameters, where each parameter is described according to a probability distribution function defining its individual uncertainty. For each set of sampled input parameters, a simulation run is made and the output quantity of interest is recorded. Typically hundreds to thousands of such sampled sets are run to collect enough statistics. Input-output correlations and standard deviations are then computed to arrive at various sensitivity coefficients and the overall output uncertainty. The details of this process are described elsewhere.[1-6] This process has been applied to aerothermal and material response codes to determine key input parameters and design margins.[1-6] A Monte Carlo analysis, although necessary, is often limited to one-dimensional or simple two-dimensional models, due to overwhelming computational cost to run thousands of simulations. Hence, a more efficient sampling scheme that reduces the sample size necessary to obtain realistic results is desirable. In this paper we use the Latin Hypercube Sampling (LHS) technique[7] to enable a more efficient Monte Carlo analysis. The LHS technique more uniformly spans the parameter hyperspace as compared to random sampling when the sample size is small. It will be shown that LHS technique can give reasonable values of output uncertainty and sensitivity ranking with a sample size that is more than an order of magnitude smaller than what is necessary with random sampling. The significant efficiency gain opens the applicability of the Monte Carlo technique to a family of more detailed (and computationally expensive) simulations. Some examples of these simulations are hypersonic lifting flight trajectories, which require full three dimensional simulations, wake dominated flows, and fully coupled simulations.

The paper presents comparisons of LHS and random sampling for a test case of a 70.2 degree sphere cone aeroshell entering the Martian atmosphere on a ballistic trajectory. The output parameter of interest is the stagnation point heat flux. The simulation is performed using the computational fluid dynamics (CFD) code called Data-Parallel Line Relaxation (DPLR)[8] for hypersonic nonequilibrium flows. The Monte Carlo analysis is performed using DAKOTA (Design Analysis Kit for Optimization and Terascale Applications).[9] Interfaces are built to enable DAKOTA to build DPLR input files, drive DPLR, and record DPLR output during the analysis. The results presented in this paper focus on the merits of LHS technique as the sample size is reduced.

2. TEST CASE AND PHYSICAL MODEL

A. Test Case: Pathfinder Entry into Mars

The test case in this paper is the Pathfinder entry vehicle, which entered the atmosphere of Mars on July 4, 1997 at at a relative velocity of 7.5 km/s.[10] Mars pathfinder is a good test case because it was a ballistic (non-lifting) entry at a velocity for which convective heating was large but radiative heating was small. The analysis in this work will be performed at the peak heating condition on the entry trajectory:[11]

$$\rho_0 = 2.8\times10^{-4}\ kg/m^3,\quad u = 6.596\ km/s,\quad T = 169\ K$$

The forebody of the Pathfinder entry vehicle was a 70.2 degree axisymmetric sphere-cone with a rounded shoulder as shown in Fig. 1.

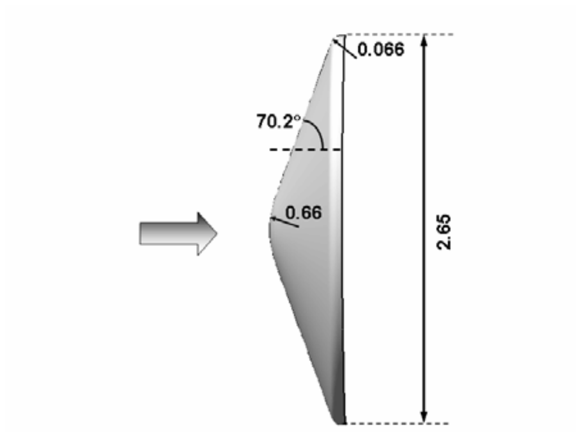

Figure 1. 72.2 degree sphere cone Mars Pathfinder aeroshell

B. Numerical and Physical Models

The flowfield computations in this work are performed using the computational fluid dynamics (CFD) code DPLR.[8] DPLR is a parallel multiblock finite-volume code that solves the Navier-Stokes equations including finite-rate chemistry and the effects of thermal nonequilibrium. DPLR is a primary tool currently used within NASA for aerothermal analysis of Earth and planetary entry vehicles. In addition to the conservation equations for mass and momentum, two energy equations are solved; a total energy equation and a combined vibro-electronic energy equation. In this formulation it is assumed that the vibrational and electronic modes of the gas are in equilibrium with each other, but not with the translational-rotational component.

Viscosity and thermal conductivity are modeled using the species expressions and mixing rules presented by Gupta et al.[12] Required collision integrals are taken from Wright et al.[13-14] for all binary interactions. The self-consistent effective binary diffusion (SCEBD) method[15] is used to model mass diffusion fluxes.

C. Chemical Kinetics Model

The Martian atmosphere consists of approximately 97% CO_2 and 3% N_2 by volume, with trace amounts of other species (primarily Ar). A review of the nonequilibrium kinetics of a shock heated mixture of CO_2–N_2 was first presented by Park *et al.*[16] for 18 species ((CO_2, NCO, CO, CO^+, CN, NO, NO^+, N_2, O_2, O_2^+, C_2, N, N^+, C, C^+, O, O^+, e) with ionization. Mitcheltree and Gnoffo[17] subsequently presented a reduced 8 species (CO_2, CO, NO, N_2, O_2, N, C, O) mechanism that neglected ionization. The reactions included in these mechanisms are listed in Table I. The rates of the common reactions are taken from Park *et al.*[16] At the conditions of interest in the present paper the level of ionization in the flowfield is extremely small. Therefore, it is expected that the heat flux computed using the Mitcheltree and Gnoffo 8-species model would be an accurate representation of the flowfield, and is used in this paper.

It should be noted that the rates of many of these reactions have not been directly measured at conditions relevant to Martian entry. Some are estimated from indirect observations, while other are pure estimates,[16] which make them sources of uncertainty.

Table 1. Reaction mechanisms for 8-species Mars entry shock layer

	Reactions
1	$CO_2 + M \Leftrightarrow CO + O + M$
2	$CO + M \Leftrightarrow C + O + M$
3	$N_2 + M \Leftrightarrow 2N + M$
4	$O_2 + M \Leftrightarrow 2O + M$
5	$NO + M \Leftrightarrow N + O + M$
6	$NO + O \Leftrightarrow O_2 + N$
7	$N_2 + O \Leftrightarrow NO + N$
8	$CO + O \Leftrightarrow O_2 + C$
9	$CO + N \Leftrightarrow NO + C$
10	$CO_2 + O \Leftrightarrow O_2 + CO$
11	$CO + NO \Leftrightarrow CO_2 + N$
12	$CO + CO \Leftrightarrow CO_2 + C$

3. METHODOLOGY

A. Analysis Procedure

A Monte Carlo sensitivity and uncertainty analysis involves statistically varying the input parameters and tracking changes in the output of interest, in this case, the stagnation point heat flux. The details of the methodology can be found in Refs. 1-4. For the sake of completeness we briefly outline the steps involved in this work.

1. Input variables that need to be varied are first identified. Based on the results of past sensitivity analysis, only two classes of input parameters are considered important and are varied: chemical kinetics rates and transport properties, which determine mass, momentum, and heat transfer across the boundary layer. Since this work focuses only on laminar, non-blowing convective heating predictions, input parameters that relate to bulk material properties, material response and turbulence models are not considered. For an 8-species kinetic model, 83 input parameters, as shown in Table II, are chosen in this work.
2. An analysis package known as DAKOTA[9] is used to sample the input parameters. DAKOTA toolkit provides the capability, via integration with a simulation tool, to perform various iterative tasks such as optimization, parameter estimation, design of experiments, sensitivity and uncertainty analysis. We vary each input parameter independently and symmetrically about their baseline values using a Gaussian distribution, width of which represents its uncertainty. The sampling scheme is either random or LHS, both options are available in DAKOTA.
3. Independent input sets generated by varying the parameters are used to make DPLR runs to obtain corresponding heat flux values.
4. Input-output correlation coefficients are computed using linear regression analysis. The overall output uncertainty is determined from the measured standard deviation of the output (i.e. stagnation heat flux).

Table 2. DPLR input parameters to be varied for sensitivity analysis

Input category	Model	Parameter varied	No. of input parameters	Mean	Std. Dev.
Dissociation reaction rates	$k=A\,T^{\eta}\exp(-D/T_a)$	$\log_{10}A$	40	Ref. 16	0.15
Exchange reaction rates	$k=A\,T^{\eta}\exp(-D/T_a)$	$\log_{10}A$	7	Ref. 16	0.15
Binary collision integral	$\Omega^{1,1},\Omega^{2,2} = Af(T)$	A	36	Refs. 13-14	10%
Total			83		

B. Sampling Technique

LHS is a more efficient sampling technique that provides better coverage over the parameter hyperspace with fewer points. In this technique the parameter hyperspace is divided in each orthogonal direction, representing each input parameter, in N_s intervals, where N_s is the sample size. The interval size is variable and is defined by the probability distribution function such that each interval occupies an equal probability region. A hypercube is constructed with the resulting grid consisting of N_s^m cells, where m is the dimension of the hyperspace. Each cell in the hypercube now represents an equal probability condition. Cells are now randomly chosen, such that each cell is picked only once, and only one cell is picked from each hyper-row (and hyper-column).

In a random sampling scheme, which has been used in the past,[1-6] sampled points are chosen at random such that their likelihood is described by the probability distribution function. In random sampling each new sample is independent of all earlier samples.

4. RESULTS AND DISCUSSION

A. Input Distribution

As discussed before, all input parameters are assumed to have Gaussian (normal) probability distribution functions, with mean and standard deviation defined in Table II. During most of the discussion, we will focus on effect of sample size on quality of results obtained using standard random sampling and the LHS scheme. Figure 2 shows distribution function of the CO_2-O transport parameter, one of the 83 input parameters sampled, as sampled by two sampling schemes. It is evident that as the sample size decreases, the distribution produced by random sampling deteriorates rapidly, while the distribution from the LHS scheme maintains an acceptable Gaussian profile. A better coverage of the parameter space with small sample sizes, especially in low probability region, is a significant advantage of the LHS scheme. These comparisons can be quantified by tabulating the mean and standard deviations measured from the sample distributions. Figure 3 shows that in almost all cases, the LHS scheme reproduces the specified mean and standard deviation better than the value reproduced by random sampling. This figure also shows, for comparison, specified mean and standard deviation of this input parameter. We also note that when smaller sample sizes are used, the values of mean and standard deviation oscillate for random sampling indicating a large statistical error. The LHS technique, on the other hand, yields stable values with small oscillations, although, the difference between specified and measured values increase steadily. Even at a large sample size of 2000, the random sampling technique is unable to produce the specified value mean and standard deviation up to 3 significant figures.

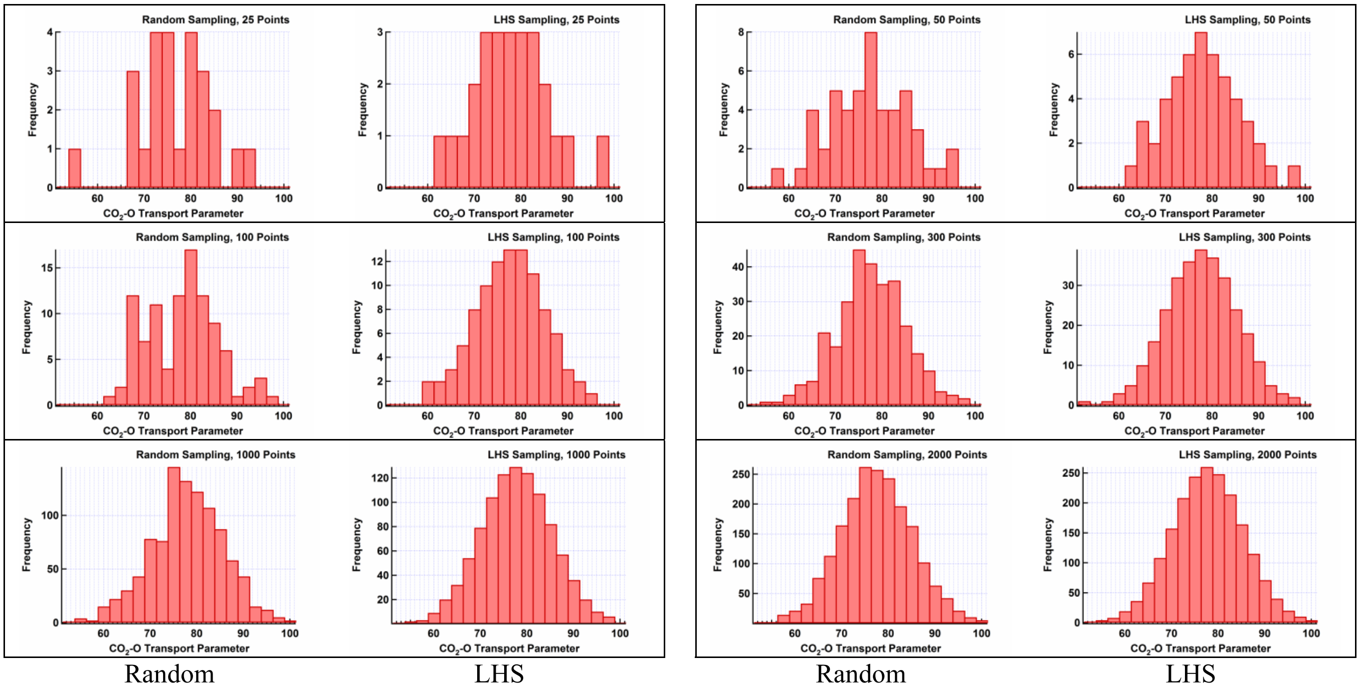

Figure 2. Comparison of sampled input distribution, specified to be a Gaussian, and its variation with sample size and sampling scheme. The LHS scheme produces better distributions at smaller sample sizes.

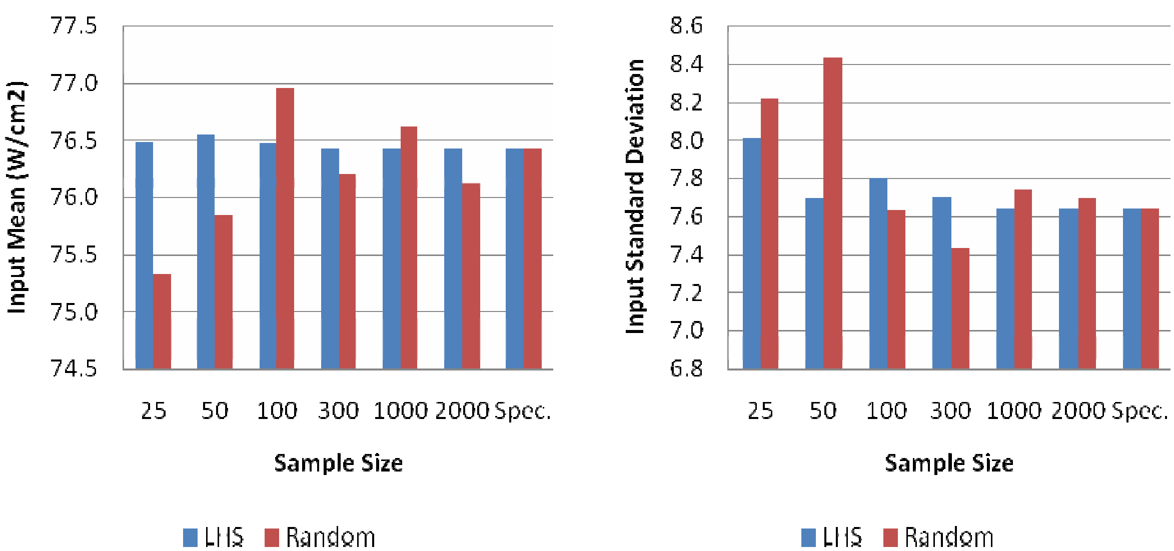

Figure 3. Mean and standard deviations of a sampled input parameter and their variation with sample size and sampling scheme. The specified mean and standard deviation are also shown.

B. Output (Stagnation Point Heat Flux) Distribution

The overall uncertainty in the output quantity of interest is a primary outcome of uncertainty analysis. This quantity determines the overall margin applied to the model prediction and could have a profound system impact. Figure 4 shows comparisons of mean and standard deviation of stagnation point heat flux. While at large sample sizes both techniques yield similar values, for sample sizes below 300, they deviate significantly. The random sampling technique shows erratic behavior due to large sampling error. The LHS technique, on the other hand, shows reasonable values for both mean and standard deviation of the output quantity of interest, even with a sample size as low as 25. The ability to obtain reasonable results with a small sample size allows this otherwise expensive technique to now be used for a wider range of complex simulations.

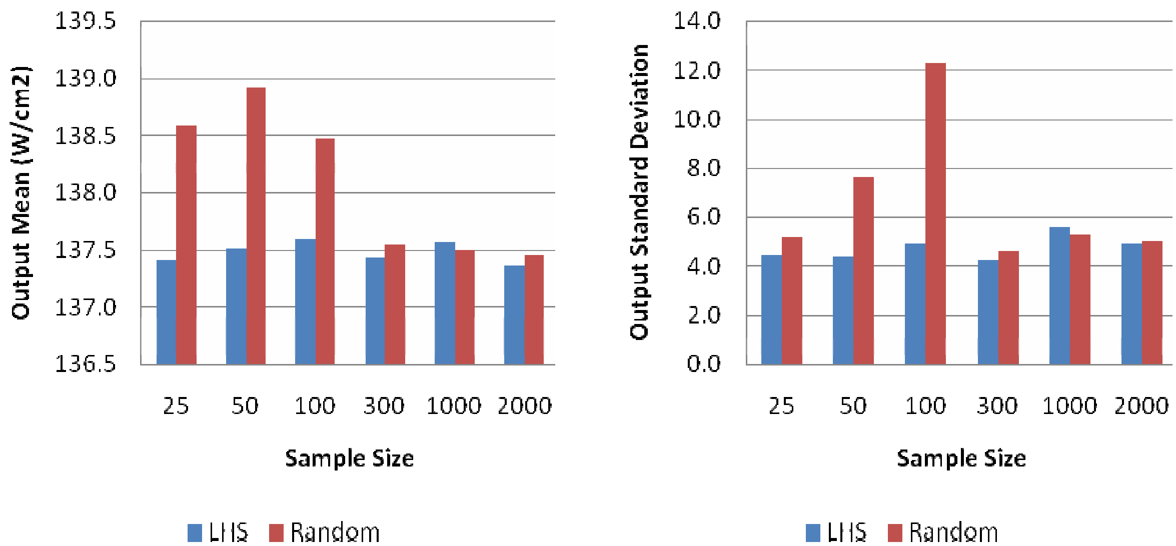

Figure 4. Mean and standard deviations of a output parameter (stagnation point heat flux) and their variation with sample size and sampling scheme.

C. Sensitivity Ranking

A sensitivity ranking is determined by listing the input parameters in descending order according to their correlation coefficients with the output quantity of interest. In this work use the linear (Pearson) correlation coefficient for sensitivity analysis. Figure 5 shows the correlation coefficients of all 83 input parameters with stagnation point heat flux. For large sample sizes we get the most reliable results as shown in Figure 5 (a sample size of 2000). In this case, only 3 out of 83 input parameters stand above all others. These three parameters are listed in Table 3.

Table 3. Three input parameters that show maximum correlation with the output quantity of interest (stagnation point heat flux).

Rank	Parameter ID	Input Parameter Definition
1	55	CO2-O Transport
2	49	CO2-CO Transport
3	62	CO-O Transport

These three parameters determine the transport of heat and mass in the boundary layer, which is primarily composed of CO_2, CO, and O. This simulation assumes that the wall is supercatalytic, which makes catalytic heating diffusion limited. This result suggests that heat transfer to the vehicle surface is limited by the collisional transfer of sensible and/or chemical energy across the boundary layer and that the edge of the boundary layer has low uncertainty. This result is insightful in that it allows the model developer to focus on key parameters to effectively target their investigation. We now seek to assess if the top-3 input parameters are identified correctly if a smaller sample size is used. Table 4 shows the sensitivity ranking obtained as the sample size is reduced. The numbers marked in red represent errors in identifying the top-3 parameters. As shown in Table 5, LHS consistently identifies the top-3 parameters correctly until the sample size is reduced below 100. The random sampling on the other hand fails to identify the order of top-3 even with a sample size of 1000. It completely misses the top-3 when the sample size is 100. This observation is further demonstrated in Fig. 6, which shows the correlation coefficients of all 83 input parameters with a sample size of 100 using both techniques.

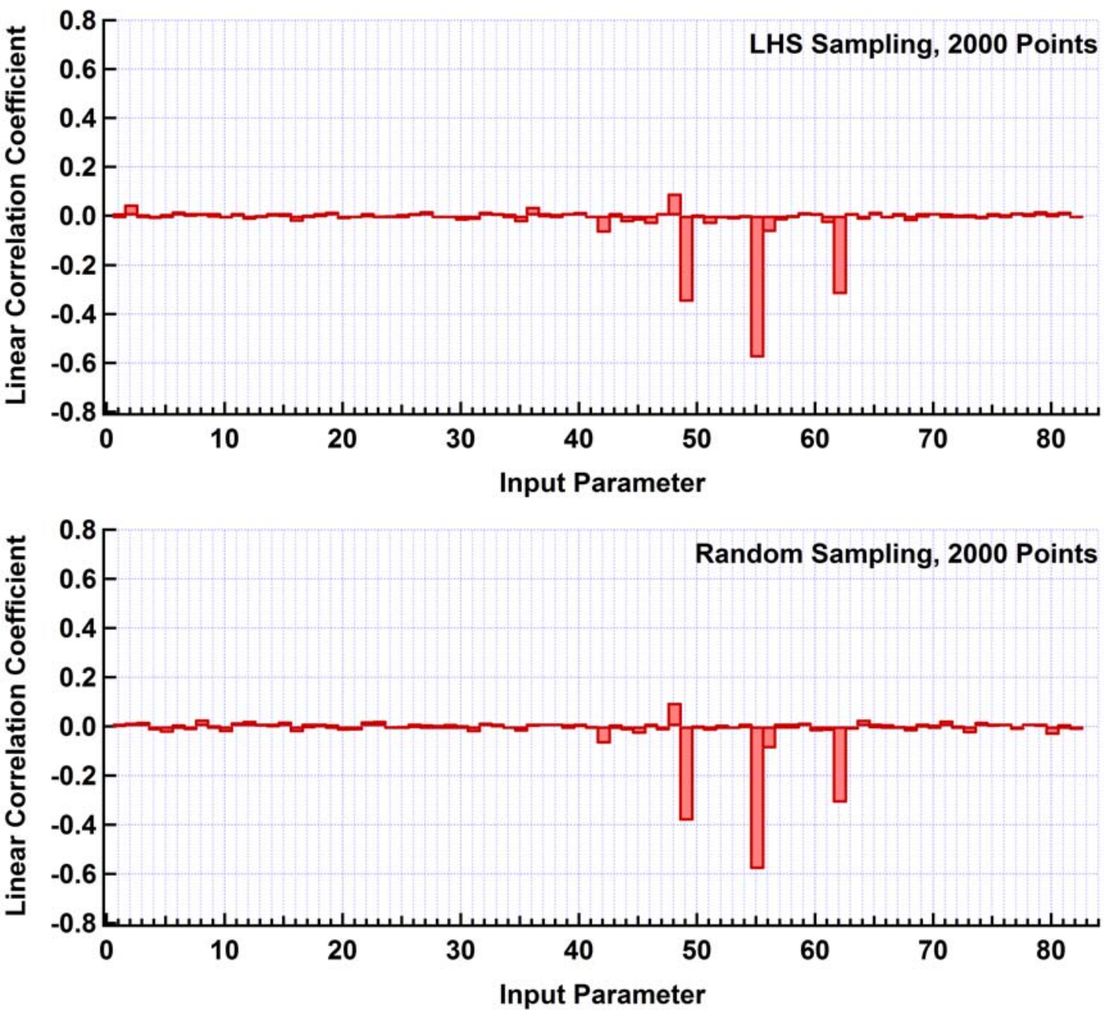

Figure 5. Input-output correlation coefficients for all 83 input parameter using a sample size of 2000. Only a handful of the parameters show reasonable sensitivity.

Table 4. Sensitivity ranking obtained by LHS and random sampling techniques. Sensitivity rankings are shown for various sample sizes. The numbers is red indicate an incorrect result due to statistical errors. The results at sample size of 2000 are assumed to be correct.

Sample Size	LHS	Random
	inp. param. id.	inp. param. id.
2000	55,49,62	55,49,62
1000	55,49,62	55,62,49
300	55,49,62	55,49,62
100	55,49,62	24,35,5
50	55,49,16	62,55,21
25	55,62,72	55,49,50

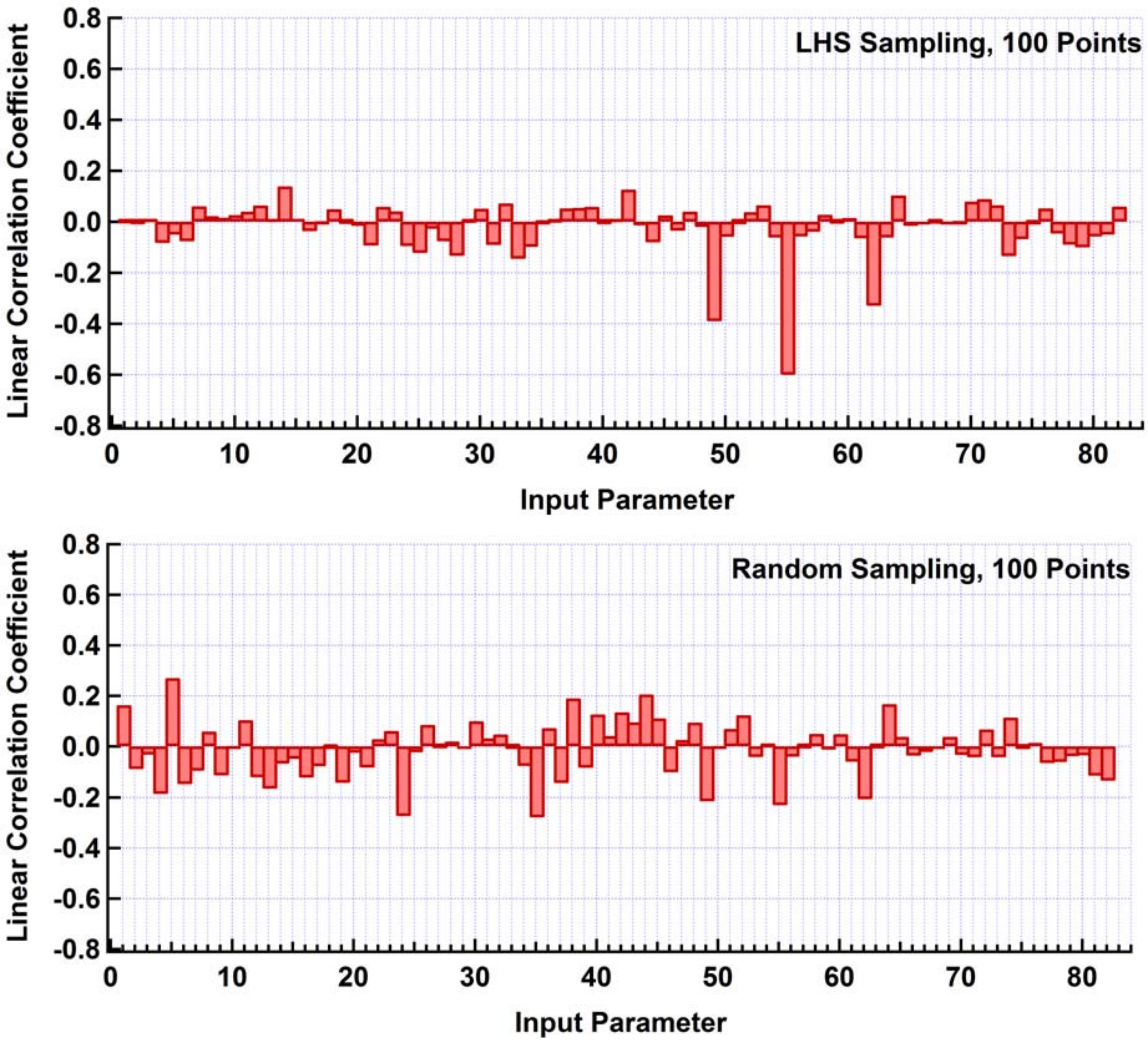

Figure 6. Input-output correlation coefficients for all 83 input parameter using a small sample size of 100. The LHS technique is still able to identify the top-3 parameters.

5. CONCLUDING REMARKS

A comparison of two different sampling schemes: random sampling and LHS, is used for Monte Carlo uncertainty analysis of aerothermal environment modeling. A test case of Mars ballistic entry was chosen to perform the analysis and compare the merits of the two sampling schemes. We find that LHS consistently reproduces values of mean and standard deviation better than the values obtained by random sampling. LHS also identifies the top-3 input parameters even with a sample size as small as 100, which represents significant savings for many applications. The ability to use a small sample size extends the applicability of this technique to more elaborate simulation more appropriate for TPS design, such as three dimensional simulations, problems with full coupling between fluid dynamics and material response, etc.

ACKNOWLEDGEMENTS

This work was partially funded by the In-Space Propulsion program under task agreement M-ISP-03-18 to NASA Ames and the CEV Thermal Protection System Advanced Development Project. The authors thank Michelle Munk (NASA LaRC) for her unwavering support of this work.

REFERENCES

[1] Dec, J.A. and Mitcheltree, R.A., "Probabilistic Design of Mars Sample Return Earth Entry Vehicle Thermal Protection System," AIAA Paper No. 2002-0910, Jan. 2002.

[2] Bose, D., Wright, M.J., and Gökçen, T., "Uncertainty and Sensitivity Analysis of Thermochemical Modeling for Titan Atmospheric Entry," AIAA Paper No. 2004-2455, Jun. 2004.

[3] Bose, D., Wright, M.J., and Palmer, G.E., "Uncertainty Analysis of Laminar Aeroheating Predictions for Mars Entries," *Journal of Thermophysics and Heat Transfer*, Vol. 20, No. 4, pp. 652-662, 2006.

[4] Wright, M.J., Bose, D., and Chen, Y.K., "Probabilistic Modeling of Aerothermal and Thermal Protection Material Response Uncertainties," *AIAA Journal,* Vol. 45, No. 2, Feb. 2007.

[5] Chen, Y.-K., Squire, T., Laub, B., and Wright, M., "Monte-Carlo Analysis for Spacecraft Thermal Protection System Design," AIAA Paper No. 2006-2951, Jun. 2006.

[6] Palmer, G.E., "Uncertainty Analysis of CEV LEO and Lunar Return Entries," AIAA-2007-4253, 39th AIAA Thermophysics Conference, Miami, FL, June 25-28, 2007.

[7] LHS paper

[8] Wright, M.J., Candler, G.V., and Bose, D., "Data-Parallel Line Relaxation Method for the Navier-Stokes Equations," *AIAA Journal*, Vol. 36, No. 9, pp 1603-1609, 1998.

[9] DAKOTA

[10] Spencer, D., Blanchard, R., B raun, R., Kallemeyn, P., and Thurman, S., "Mars Pathfinder Entry, Descent and Landing Reconstruction," *Journal of Spacecraft and Rockets*, Vol. 36, No. 3, 1999, pp. 357-366.

[11] Milos, F. S., Chen, Y.-K., Congdon, W.M., and Thornton, J.M., "Mars Pathfinder Entry Temperature Data, Aerothermal Heating, and Heatshield Material Response," *Journal of Spacecraft and Rockets*, Vol. 36, No. 3, pp. 380-391, 1999.

[12] Gupta, R., Yos, J., Thompson, R., and Lee, K., "A Review of Reaction Rates and Thermodynamic and Transport Properties for an 11-Species Air Model for Chemical and Thermal Nonequilibrium Calculations to 30000 K," NASA RP-1232, Aug. 1990.

[13] Wright, M.J., Hwang, H.H., and Schwenke, D.W., "Recommended Collision Integrals for Transport Property Computations II: Mars and Venus Entries," *AIAA Journal*, Vol. 45, No. 1, 2007, pp. 281-288.

[14] Wright, M.J., Bose, D., Palmer, G.E., and Levin E., "Recommended Collision Integrals for Transport Property Computations I: Air Species," *AIAA Journal*, Vol. 43, No. 12, 2005, pp. 2558-2564.

[15] Ramshaw, J.D., "Self-Consistent Effective Binary Diffusion in Multicomponent Gas Mixtures," *Journal of Non-Equilibrium Thermodynamics*, Vol. 15, No. 3, 1990, pp. 295-300.

[16] Park, C., Howe, J.T., Jaffe, R.L., and Candler, G.V., "Review of Chemical-Kinetic Problems of Future NASA Missions, II: Mars Entries," *Journal of Thermophysics and Heat Transfer*, Vol. 8, No. 1, pp. 9-23, 1994.

[17] Mitcheltree, R.A., and Gnoffo, P.A., "Wake Flow about the Mars Pathfinder Entry Vehicle," *Journal of Spacecraft and Rockets*, Vol. 32, No. 5, pp. 771-776, 1995.

Paper No. 14

Discusser's Name: Bil Kleb

Question: How do you accommodate input parameters with realizability constraints, e.g. A ε [0, 1]?

Authors' Reply: It depends on the physical parameter. In general we use a uniform distribution or employ a best and worst case scenario.